AD-754 032

PRACTICAL DIGITAL FILTER DESIGN

Patrick H. Garrett

Ohio University

Prepared for:

Army Electronics Command

October 1972

Research and Development Technical Report

ECOM-0084-S-6

PRACTICAL DIGITAL FILTER DESIGN

By
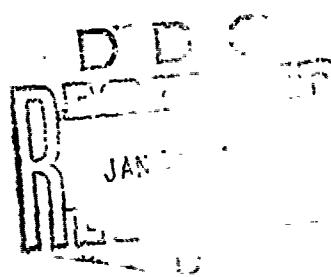
Patrick H. Garrett

October 1972

DISTRIBUTION STATEMENT
Approved for public release:
Distribution unlimited.

ECOM

UNITED STATES ARMY ELECTRONICS COMMAND · FORT MONMOUTH, N.J.

NOTICES

Disclaimers

Disposition

DOCUMENT CONTROL DATA - R & D

(Security classification of title, body of abstract and indexing annotation must be entered when the overall report is classified)

1. ORIGINATING ACTIVITY (Corporate author)	2a. REPORT SECURITY CLASSIFICATION
Avionics Research Group	UNCLASSIFIED
Department of Electrical Engineering	2b. GROUP
Ohio University, Athens, Ohio 45701	

3. REPORT TITLE

PRACTICAL DIGITAL FILTER DESIGN

4. DESCRIPTIVE NOTES (Type of report and inclusive dates)

5. AUTHOR(S) (First name, middle initial, last name)

Patrick H. Garrett

6. REPORT DATE	7a. TOTAL NO. OF PAGES	7b. NO. OF REFS
October 1972	36	4

8a. CONTRACT OR GRANT NO.	9a. ORIGINATOR'S REPORT NUMBER(S)
DAAB07-68-C-0084	ECOM-0084-S -6
b. PROJECT NO.	
c.	9b. OTHER REPORT NO(S) (Any other numbers that may be assigned this report)
d.	TR EER 16-15

10. DISTRIBUTION STATEMENT

Approved for Public Release; Distribution Unlimited

11. SUPPLEMENTARY NOTES	12. SPONSORING MILITARY ACTIVITY
	US Army Electronics Command
	ATTN: AMSEL-VL N
	Fort Monmouth, New Jersey 07703

13. ABSTRACT

Review of Fourier, Laplace and Z-transforms provides introduction to discrete time systems. The RC low-pass filter is modeled in terms of a feedback structure and compared with its analogy to recursive low-pass digital filters. These topics introduce the preferred transversal digital filter for low-pass and band-pass applications. An efficient method of synthesizing transversal filters is demonstrated from the derivation of Fourier coefficients and time delays. A method of weighting the truncated Fourier terms by Hamming coefficients to suppress Gibb's oscillation is also shown. Design examples demonstrating the magnitude and phase response of low-pass and band-pass transversal filters are presented.

14. KEY WORDS	LINK A		LINK B		LINK C	
	ROLE	WT	ROLE	WT	ROLE	WT
Fourier transforms						
Laplace transforms						
Z-transforms						
Recursive digital filters						
Transversal digital filters						
Fourier coefficient derivation						
Digital filter coefficient synthesis						
Hamming weighted coefficients						
Low-pass digital filters						
Band-pass digital filters						
Magnitude and phase example responses						

PRACTICAL DIGITAL FILTER DESIGN

·Prepared by

Patrick H. Garrett

Avionics Research Group
Department of Electrical Engineering
Ohio University
Athens, Ohio 45701

For

TABLE OF CONTENTS

LIST OF FIGURES

INTRODUCTION

The rise of digital filtering has come about as a result of two factors which are not totally independent. The first is traceable to the fact that more process cc .rol and signal processing operations are now being executed digitally which were previously accomplished in the analog domain. Once signals are in a digital format, it is obviously more efficient to complete all necessary operations digitally. The second factor bringing about a more widespread application of digital filters is the continuing decrease in cost per digital hardware function. This is due to a 'vances in the state-of-the-art and economic factors of high volume production. Digital filters, therefore, may be realized with either software as a part of a larger executive program, or in a hardwired hardware form, with perhaps A/D and D/A input and output converters, to accomplish a specific filtering task.

The decision of when to use digital filters instead of, for example, active-type analog filters is not dictated by hard-and-fast guidelines. This decision is strictly dependent upon the application at hand. The principal features of digital filters are high stability and the ease with which filter parameters can be changed. The former is useful for separating signals very close in frequency and where the filter must be located in other than ideal environments. The latter feature is essential for adaptive filtering where a filter must change its characteristics in real-time to a changing input signal. The following development presents the essentials of digital filtering from a practical viewpoint which the practicing engineer can immediately put to use and includes both low-pass and band-pass design examples with their output response plots.

1 -

FOURIER TRANSFORMS

The Fourier transform pair is useful for transforming functions between the time and frequency domains

$$g(\omega) = \int_{-\infty}^{\infty} f(t) \cdot e^{-j\omega t} \, dt$$

$$f(t) = \frac{1}{2\pi} \int_{-\infty}^{\infty} g(\omega) \cdot e^{j\omega t} \, d\omega$$

Consider a single pulse of amplitude A and width τ. Its transform from the time to frequency domains provides the spectral density of the pulse. It can be seen that a pulse of width τ requires a bandwidth of $2/\tau$ Hertz for transmission or re-production with fidelity since the majority of the energy contained within the pulse is seen to lie between $\pm 1/\tau$ Hertz of the spectral density plot.
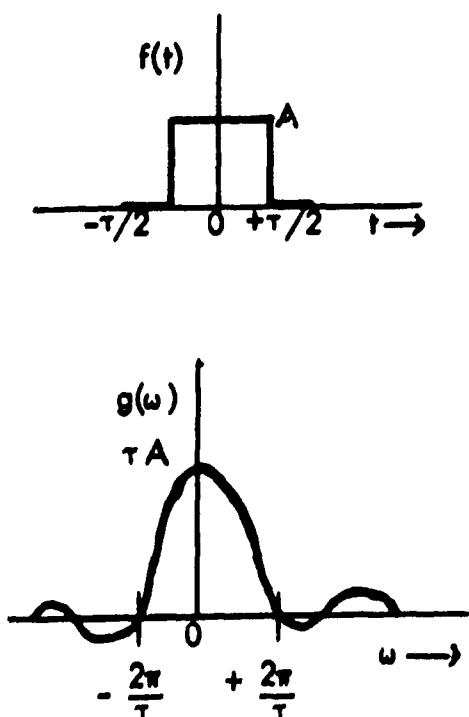
$$g(\omega) = \int_{-\tau/2}^{\tau/2} A \cdot e^{-j\omega t} \, dt$$

$$= \frac{-A}{j\omega} e^{-j\omega t} \Big|_{-\tau/2}^{\tau/2}$$

$$= A \frac{e^{j\omega\tau/2} - e^{-j\omega\tau/2}}{j\omega}$$

$$= \tau A \frac{\sin(\omega\tau/2)}{(\omega\tau/2)}$$

LAPLACE TRANSFORMS

The Laplace transform pair is a one-sided Fourier transform pair useful for transforming discontinuous functions between the time and frequency domains which the Fourier transforms cannot handle. For example, consider a Fourier transform of a unit step function

$$g(\omega) = \int_{0}^{\infty} 1 \cdot e^{-j\omega t} \, dt$$

$$= \frac{-1}{j\omega} e^{-j\omega t} \Bigg|_{0}^{\infty}$$

$$= \frac{-1}{j\omega} (\cos \infty - j \sin \infty - 1)$$
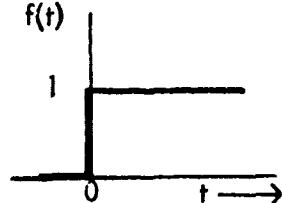
This result is undefined and therefore meaningless. However, convergence of this integral can be assured by adding a constant σ to $j\omega$ providing $s = \sigma + j\omega$, which is a complex variable. Considering now the Laplace transform of a unit step function we obtain a useful solution
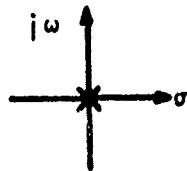
$$g(\sigma + j\omega) = \int_{0}^{\infty} 1 \cdot e^{-(\sigma + j\omega)t} \, dt$$

$$= \frac{-1}{\sigma + j\omega} e^{-(\sigma + j\omega)t} \Bigg|_{0}^{\infty}$$

$$= \frac{1}{\sigma + j\omega}$$

The Laplace transform pair is therefore given by

$$g(\sigma + j\omega) = F(s) = \int_{0}^{\infty} f(t) \cdot e^{-st} \, dt$$

$$\mathcal{L}^{-1}[F(s)] = F(t) = \int_{\sigma - j\omega}^{\sigma + j\omega} F(s) \cdot e^{st} \, ds$$

Z - TRANSFORMS

Laplace transforms are principally useful for continuous functions. If the
Laplace transform of a time-sampled continuous function is considered

$$F(s) = \int_0^\infty f(t)\, e^{-st}\, dt$$

$$= \int_0^\infty [\sum_{n=0}^\infty f(t)\, \delta\,(t-nT)]\, e^{-st}\, dt$$

$$= \sum_{n=0}^\infty \int_0^\infty [f(t)\, e^{-st}]\, \delta\,(t-nT)\, dt$$

$$= \sum_{n=0}^\infty f(nT)\, e^{-nsT}$$

The final expression evaluates each time $t = nT$. For convenience we define a unit
time delay operator $z^{-1} = e^{-sT}$ which provides the Z-transform pair

$$F(z) = \sum_{n=0}^\infty f(nT)\, Z^{-n}$$

$$f(nT) = \frac{1}{2\pi j} \int F(z)\, Z^{n-1}\, dz$$

RC LOW PASS FILTER

Both an analog and digital realization of a single-section RC filter will be considered as an illustration of an intuitive approach to digital filter design.
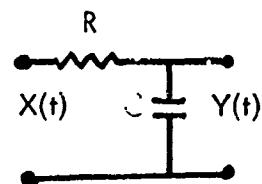
$$T(t) = \frac{Y(t)}{X(t)} = \frac{1/j\omega c}{R + 1/j\omega c}$$

$$= \frac{1}{1 + j\omega RC}$$

$$T(s) = \frac{Y(x)}{X(s)} = \frac{1}{1 + RCS}$$

Recalling that the transfer function for a feedback structure is given by $T = G/(1+GH)$, we represent the analog RC filter in like manner

- 6 -
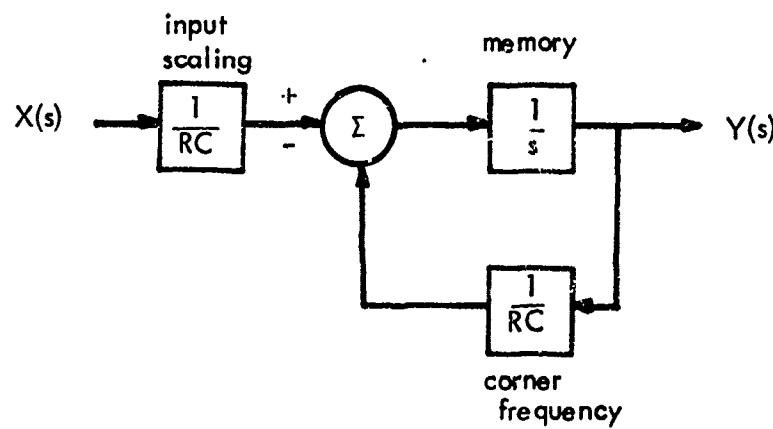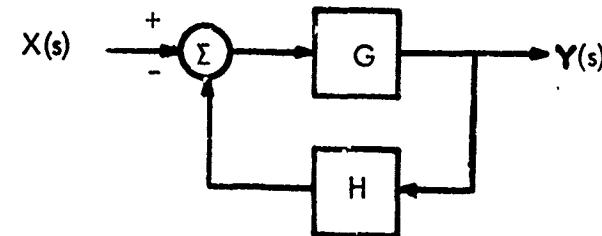
Consider now filter excitation by a unit step function beginning at $t = 0$. The resulting RC filter output response is obtained with the aid of Laplace transforms of this input step and the filter transfer function

$$X(s) = \int_0^\infty 1 \cdot e^{-st} \, dt$$

$$= \frac{1}{s}$$
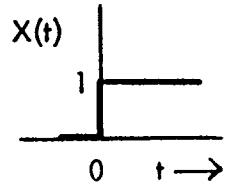
$$Y(s) = X(s) \cdot T(s)$$

$$= \frac{1}{s} \cdot \frac{1}{1 + RCS}$$

Expansion of $Y(s)$ by partial fractions and obtaining the inverse Laplace transform from tables yields the RC filter output time response in terms of an exponential function

$$Y(s) = \frac{1}{s} - \frac{1}{s + 1/RC}$$

$$Y(t) = \mathcal{L}^{-1} [Y(s)]$$

$$= 1 - e^{-t/RC}$$
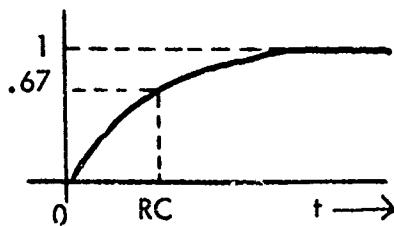
RECURSIVE DIGITAL FILTERS

The foregoing single-section RC filter may also be realized in digital form by obtaining the Z-transform of the input step function and the just presented output time response $Y(t)$. The transfer function formed with these quantities is also realizable with a recursive feedback structure as shown for the analog case.

$$X(z) = \sum_{n=0}^{\infty} X(nT) Z^{-n}$$

$$= \sum_{n=0}^{\infty} 1 \cdot Z^{-n}$$

$$= \frac{1}{1 - Z^{-1}}$$

$$Y(z) = \sum_{n=0}^{\infty} Y(nT) Z^{-n}$$

$$= \sum_{n=0}^{\infty} (1 - e^{-nT/RC}) Z^{-n}$$

$$= \sum_{n=0}^{\infty} 1 \cdot Z^{-n} - \sum_{n=0}^{\infty} e^{-nT/RC} Z^{-n}$$

$$= \frac{1}{1 - Z^{-1}} - \frac{1}{1 - e^{-T/RC} Z^{-1}}$$

The transfer function $T(z)$ and its realization are

$$T(z) = \frac{Y(z)}{X(z)} = \frac{Z^{-1}(1 - e^{-T/RC})}{(1 - e^{-T/RC} Z^{-1})}$$
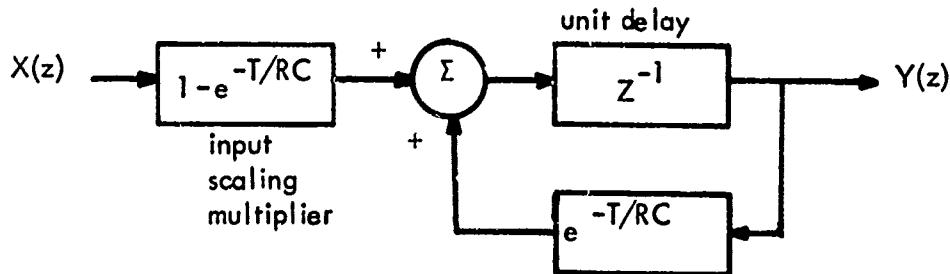
The foregoing introduction is meant to bridge the gap between continuous-function analog filters and sampled-function digital filters. The particular example chosen is intended as a simple exercise rather than a practical example of digital filter design. Recursive filter designs are feasible only under rather severe realizability constraints. The details of these constraints can only be briefly addressed here. However, since they are feedback structures recursive filters are subject to all of the stability considerations of analog feedback systems plus additional ones which can defy practical solution. For example, quantization noise encountered in the sampling process when fedback and multiplied by the various filter coefficients can produce non-linear behavior and filter limit cycling. In addition, passband phase shift in recursive filters is generally difficult to linearize and/or compensate satisfactorily. A more practical and useful approach to digital filters is possible with the transversal structure. For the above stated reasons the following development is devoted to a detailed presentation of transversal digital filter design.

TRANSVERSAL DIGITAL FILTERS

The transversal filter, also known as a finite-memory or nonrecursive filter, is not suitable for integration applications due to this availability of only a finite memory. However, it is useful for low-pass filtering, interpolation and extrapolation (delay and prediction), differentiation and combinations of the above. In addition, and to be introduced subsequently, with the low-pass to band-pass transformation the transversal filter mechanization provides a band-pass filter with all of the advantages represented by transversal filters.

Digital filtering of continuous signals involves the signal processing operations of sampling and quantization, which is addressed elsewhere in this treatise, as well as the computational operations of storage, multiplication and addition. Digital filters can be made to approximate their RLC counterparts insofar as conforming to the Butterworth, Bessel, or Chebyshev characteristics, for example, if this is of interest. However, a more direct approach is elected in this presentation whereby we will be concerned with considerations of passband, transition regions, stopband, ripple and phase. This direct approach will provide more insight into the design of digital filters without manipulating esoteric transfer functions in order to achieve particular response characteristics.

Low-pass transversal digital filter structures are useful for estimating, at discrete time instants, the value of a random signal perturbed by additive noise. Transversal filters are always stable since no feedback paths are involved and designs with exactly linear phase are easily realized. In addition, due to this inherent stability coefficient

value approximations may be relaxed which permits shorter coefficient multiplier word-lengths. This plus the fact that only a finite number of states are generally required for a transversal filter realization provides efficiency in its hardware mechanization. The spectral response in the Z-domain of a transversal filter is expressed by Equation (1) and its block diagram by Figure 1.

$$H(z) = \sum_{n=0}^{\infty} a_n Z^{-n} \tag{1}$$
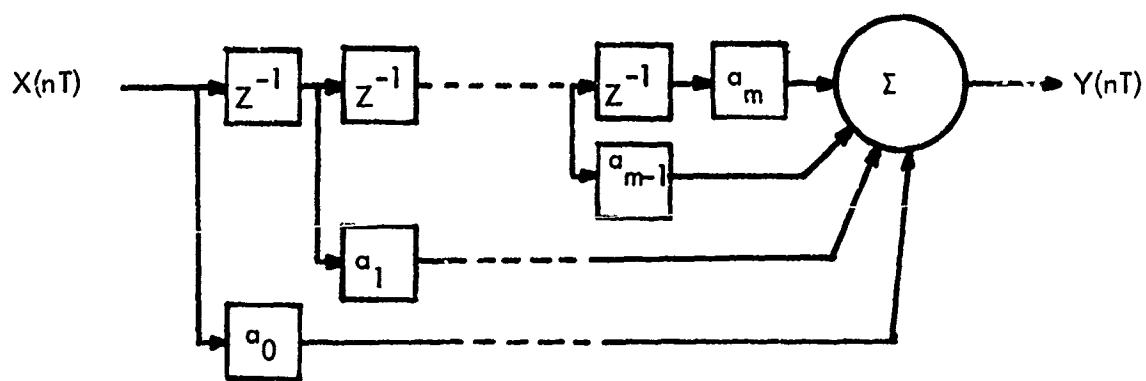
Figure 1. Transversal Filter Mechanization

LOW PASS TRANSVERSAL FILTERS

Consider now the design of a low pass filter whose frequency response is in general represented by Figure 2. In radians per second, ω_c is the filter cutoff frequency, ω_{stop} the frequency where high attenuation exists, and ω_s the filter sampling, computation and Z^{-1} delay rate which in practice is selected sufficiently high to satisfy the Nyquist Sampling Theorem and to prevent overlap of the periodic

- 11 -

spectrum foldover. This will be addressed in sufficient detail at the appropriate point later.
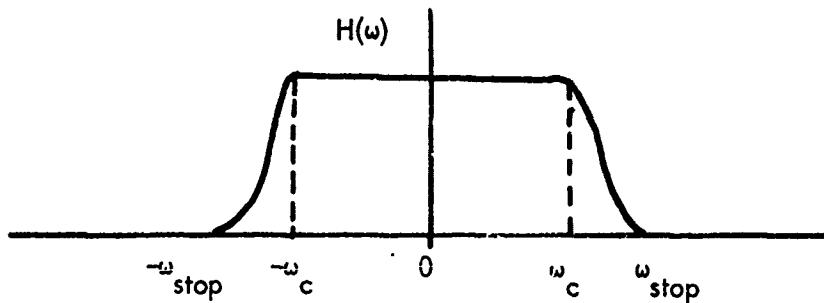
Figure 2. Frequency Domain Filter Response

The designer initially determines the allowable filter transition region between the passband and the stopband which is given by Equation (2)

$$\omega_{stop} - \omega_c = \Delta \omega \tag{2}$$

Since there are no signal components passed by the filter at frequencies above ω_{stop}, then the filter output must drop from its passband value at ω_c to the desired attenuation at ω_{stop}. Filter rolloff in terms of DB/decade or DB/octave is therefore easily specified. Note that no comment was made about how many DB down the filter response will be at the cutoff frequency. This is because it is not necessary to impose the parametric characteristics of analog RLC filters on digital filter designs. As we will see shortly, response factors are determined by parameters alien to analog filter design. Before discussing this, however, the Fourier-series method for obtaining the filter multiplier coefficients, a_n of Figure 1, will be presented.

- 12 -

The frequency response of the transversal filter defined by Equation (1) may be found by the substitution shown in Equation (3) which provides the frequency domain filter response of Equation (4)

$$Z = e^{st} \Big|_{s = j\omega} = e^{j\omega T} \tag{3}$$

$$H(\omega) = \sum_{n=0}^{m} a_n e^{-jn\omega T} \tag{4}$$

$H(\omega)$ may then be divided into its real and imaginary parts described below

$$H(\omega) = U(\omega) + j V(\omega) \tag{5}$$

$$U(\omega) = a_o + \sum_{n=1}^{\infty} a_n \cos n\omega T \tag{6}$$

$$V(\omega) = \sum_{n=1}^{\infty} \beta_n \sin n\omega T \tag{7}$$

We may also write these terms in the form of their exponential equivalent

$$U(\omega) = a_o + \frac{1}{2} \sum_{n=1}^{\infty} a_n (e^{jn\omega T} + e^{-jn\omega T}) \tag{8}$$

$$j V(\omega) = \frac{1}{2} \sum_{n=1}^{\infty} \beta_n (e^{jn\omega T} - e^{-jn\omega T}) \tag{9}$$

In practice, the series is truncated symmetrically for economy of implementation. This yields a total of $2J+1$ filter states, where $m=2J$. The Z-domain expression for the transversal filter in terms of Fourier coefficients is given by Equations (10) and (11)

$$H(z) = a_o + \frac{1}{2} \left[\sum_{n=1}^{J} (a_n - \beta_n) Z^{-n} + \sum_{n=1}^{J} (a_n + \beta_n) Z^n \right] \tag{10}$$

$$= \sum_{n=0}^{2J} a_n Z^{-n} \tag{11}$$

The filter coefficient multipliers are specifically given by

$$a_o = \frac{1}{2}(a_J + \beta_J)$$

$$a_1 = \frac{1}{2}(a_{J-1} + \beta_{J-1})$$

$$\vdots \qquad \vdots$$

$$a_{J-1} = \frac{1}{2}(a_1 + \beta_1)$$

$$a_J = a_o$$

$$a_{J+1} = \frac{1}{2}(a_1 - \beta_1)$$

$$\vdots \qquad \vdots$$

$$a_{m-1} = \frac{1}{2}(a_{J-1} - \beta_{J-1})$$

$$a_m = \frac{1}{2}(a_J - \beta_J)$$

If the Fourier series is truncated using a rectangular window as indicated by Equations (10) and (11) and the resu'ing filter multiplier coefficients, the filter frequency response will exhibit Gibb's oscillation due to the discontinuity in $H(\omega)$. Gibb's oscillation can be effectively reduced by modifying the Fourier coefficients by means of a weighting function. The Hamming window is particularly useful for controlling the ripple in the frequency response of finite-length sequences. A function describing this window is presented by Equation (12)

$$W_{H(n)} = \begin{cases} 0.54 + 0.46 \cos\left(\frac{\pi n}{J}\right) & n \leq J \\ 0 & n > J \end{cases} \tag{12}$$

Use of the Hamming weighting function provides not only control of the ripple, but specifies the optimum truncated filter sequence length J in terms of the desired filter transition region $\Delta \omega$. Sampling time T is defined in terms of the sampling frequency ω_s, where $T = 2\pi/\omega_s$.

$$J = \frac{2\pi}{T\Delta \omega} \tag{13}$$

The Hamming weighted filter coefficient multipliers are then given by

$$a_o = \tfrac{1}{2} W_{(J)} (\alpha_J + \beta_J)$$

$$a_1 = \tfrac{1}{2} W_{(J-1)} (\alpha_{J-1} + \beta_{J-1})$$

$$\vdots \qquad\qquad \vdots$$

$$a_{J-1} = \tfrac{1}{2} W_{(1)} (\alpha_1 + \beta_1)$$

$$a_J = a_o$$

$$a_{J+1} = \tfrac{1}{2} W_{(1)} (\alpha_1 - \beta_1)$$

$$\vdots \qquad\qquad \vdots$$

$$a_m = \tfrac{1}{2} W_{(J)} (\alpha_J - \beta_J)$$

The Fourier coefficients are obtained by noting that the filter response in the frequency domain is periodic at a foldover repetition frequency defined by the sampling frequency ω_s. From Figure 3 it can be seen that in order to prevent overlap of the periodic spectrums, ω_s must be sufficiently high to assure adequate spacing. A rule-of-thumb is that ω_s is taken at two to ten times the highest frequency of interest. If overlap is allowed to occur, the phenomenon of aliasing will take place producing errors in the reconstruction of a continuous signal at the output from its sampled representation.
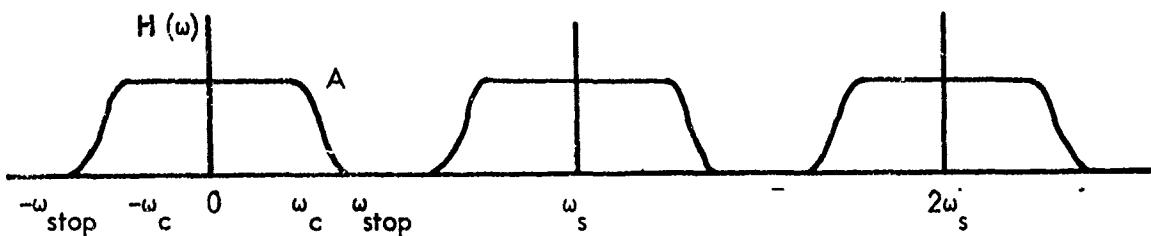
Figure 3. Periodic Spectrum Foldover

Due to the even symmetry imposed by the spectral response of $H(\omega)$ about zero for the low-pass filter, all of the β_n terms will be zero. This leaves the DC and even α_n terms to be evaluated. Considering $\omega_s/2 = \pi/T$ we then write

$$\beta_n = \frac{2}{\omega_s} \int_{-\omega_c}^{+\omega_c} A \cdot \sin \left(n \frac{2\pi}{\omega_s} \omega \right) d\omega = 0 \qquad (14)$$

$$\alpha_o = \frac{2\omega_c}{\omega_s} \qquad (15)$$

$$\alpha_n = \frac{2}{\omega_s} \int_{-\omega_c}^{+\omega_c} A \cdot \cos \left(n \frac{2\pi}{\omega_s} \omega \right) d\omega \qquad (16)$$

Evaluating these expressions in the frequency domain with a normalized amplitude $A = 1$ yields

$$\alpha_n = \frac{2}{\omega_s} \int_{-\omega_c}^{\omega_c} 1 \cdot \cos(n \omega T) d\omega$$

$$= \frac{T}{\pi} \int_{-\omega_c}^{\omega_c} \frac{1}{nT} \cdot nT \cdot \cos(n \omega T) d\omega$$

$$= \frac{2}{n\pi} \sin(n \omega_c T) \qquad (17)$$

- 16 -

LOW PASS DESIGN EXAMPLE

Consider a low-pass filter cutoff frequency of 1 Hz, or $\omega_c = 2\pi$. Such a filter could be applicable to thermocouple inputs at a data logging station. A sample frequency must then be chosen to be greater than twice the highest frequency of interest ω_{stop}. For a selected transition region of $\Delta\omega = 2\pi$ the filter has an $\omega_{stop} = 4\pi$. A value for $\omega_s = 16\pi$ is then selected as two times the minimum practical sampling frequency for this filter. Then, $T = 2\pi/\omega_s = 1/8$ second and the number of required filter states to realize this filter is obtained from Equations (18) and (19). The Fourier DC and even coefficients are found, respectively, by Equations (20) and (21)

$$J = \frac{2\pi}{T\Delta\omega} = 8 \tag{18}$$

$$m = 2J = 16 \tag{19}$$

$$\alpha_o = \frac{2\omega_c}{\omega_s} = 1/4 \tag{20}$$

$$\alpha_n = \frac{2}{n\pi} \cdot \sin\left(\frac{n\pi}{4}\right) \tag{21}$$

The Fourier and Hamming coefficients for this filter are then obtained from Equations (21) and (16) as

FOURIER	HAMMING
$\alpha_1 = +0.462$	$W_{H1} = +1.44$
$\alpha_2 = +0.318$	$W_{H2} = +1.16$
$\alpha_3 = +0.150$	$W_{H3} = +0.76$
$\alpha_4 = 0.0$	$W_{H3} = +0.25$
$\alpha_5 = -0.090$	$W_{H5} = -0.09$
$\alpha_6 = -0.106$	$W_{H6} = -0.36$
$\alpha_7 = -0.064$	$W_{H7} = -0.46$
$\alpha_8 = 0.0$	$W_{H8} = -0.35$

The 17 filter multiplier coefficients weighted by the rectangular (simple truncation) and Hamming windows are

HAMMING	RECTANGULAR
$a_0, a_{16} = 0.0$	$a_0, a_{16} = 0.0$
$a_1, a_{15} = +0.0147$	$a_1, a_{15} = -0.032$
$a_2, a_{14} = +0.0191$	$a_2, a_{14} = -0.053$
$a_3, a_{13} = +0.0040$	$a_3, a_{13} = -0.045$
$a_4, a_{12} = 0.0$	$a_4, a_{12} = 0.0$
$a_5, a_{11} = +0.0570$	$a_5, a_{11} = +0.075$
$a_6, a_{10} = +0.1845$	$a_6, a_{10} = +0.159$
$a_7, a_9 = +0.3325$	$a_7, a_9 = +0.231$
$a_8 = +0.25$	$a_8 = +0.25$

The magnitude and phase response of the low-pass digital filters implemented with the preceding Hamming and rectangularly weighted multiplier coefficients were obtained from the following frequency-domain equations

$$H(\omega) = \sum_{n=0}^{m} a_n e^{-jn\omega T}$$

$$= \sum_{n=0}^{m} a_n \left[\cos(n\omega T) - j \sin(n\omega T) \right] \tag{22}$$

$$\Phi = \tan^{-1} \frac{\sin(\omega T)}{\cos(\omega T)} \tag{23}$$

A computer generated plotting routine was executed with these equations for $T = 1/8$ with ω ranging from 0 to 4π and $m = 16$. Figures 4 through 7 present these results.

Consider the Hamming weighted filter of Figure 4. The attenuation achieved between the passband magnitude of 1.47 and the stopband ripple peak of 0.15 is a ratio of 10, or 20 DB. The transition region, however, extends over 1.25 Hertz

- 18 -

instead of the predicted 1 Hertz. In addition, the cutoff frequency of 1 Hertz is centered about halfway along the transition region instead of at the beginning as expected. These anomalies are primarily due to an insufficient sampling rate. Referring to Equation (18), it can be seen that for the specified transition region of 1 Hertz that a higher sampling rate, implicit in a smaller T, will provide additional Fourier coefficients and hence filter states to better approximate the desired response. The phase response of this filter, presented by Figure 5, is linear and well behaved even at this minimum sampling rate. The magnitude and phase response for the digital filter formulated from rectangularly truncated Fourier coefficients is shown by Figures 6 and 7. The behavior of this filter departs from the Hamming-weighted filter primarily in terms of the undesired Gibb's oscillation it exhibits in the passband. Illustration of this oscillation, of course, is the purpose for providing this comparison.
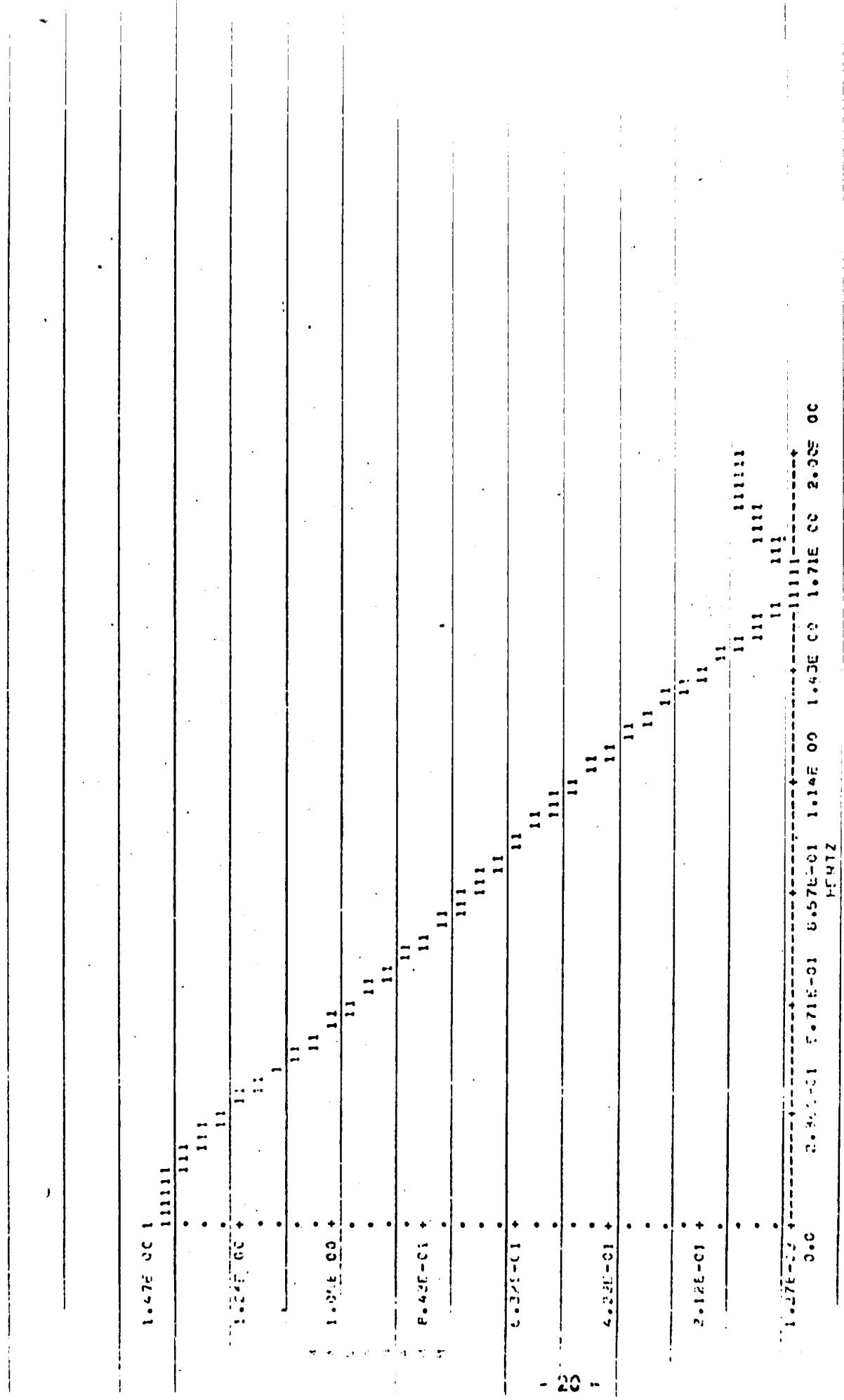
Figure 4. Hamming Weighted Filter Magnitude Response

- 20 -
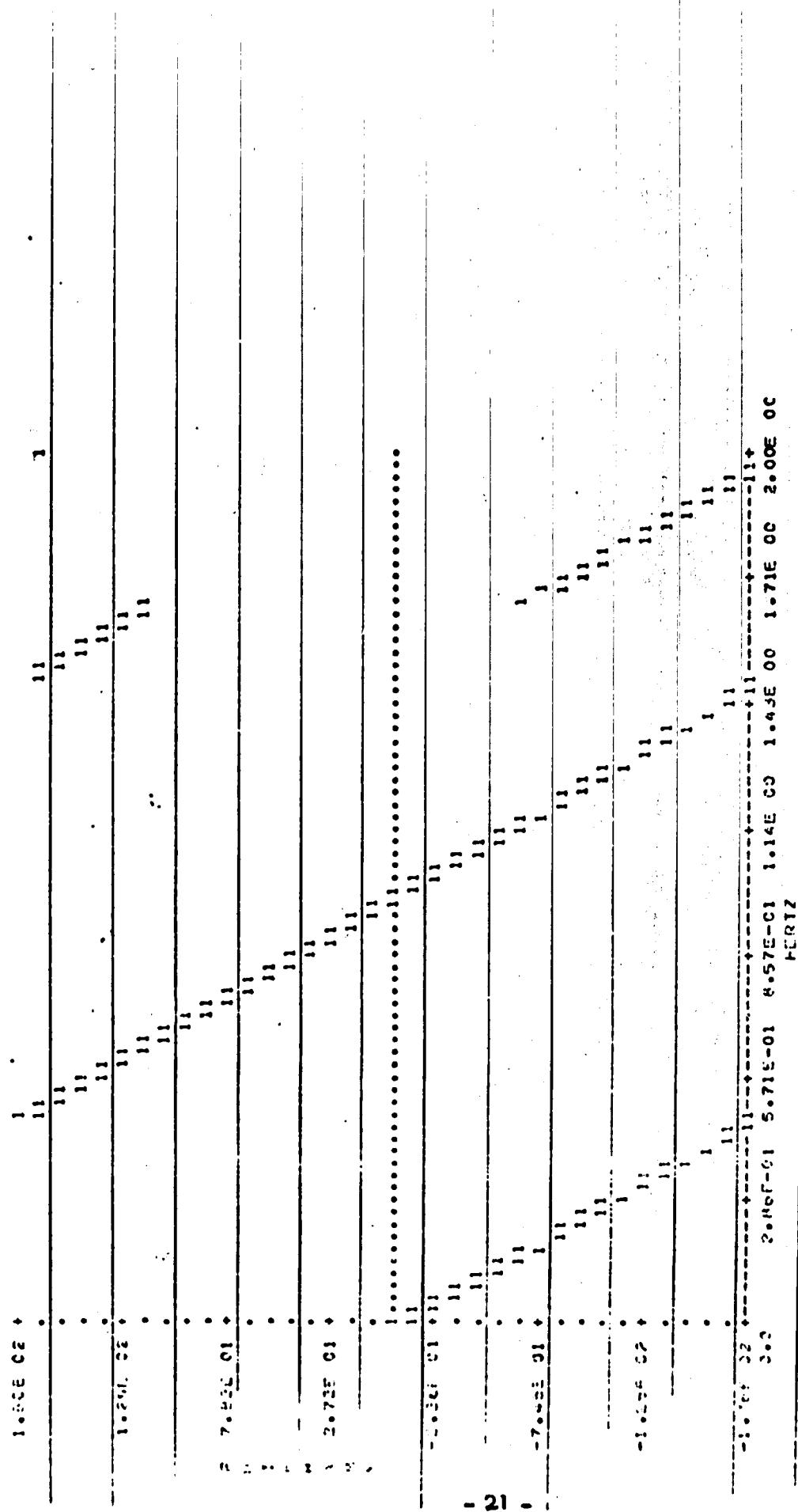
Figure 5. Hamming Weighted Filter Phase Response

Figure 6. Rectangularly Weighted Filter Magnitude Response
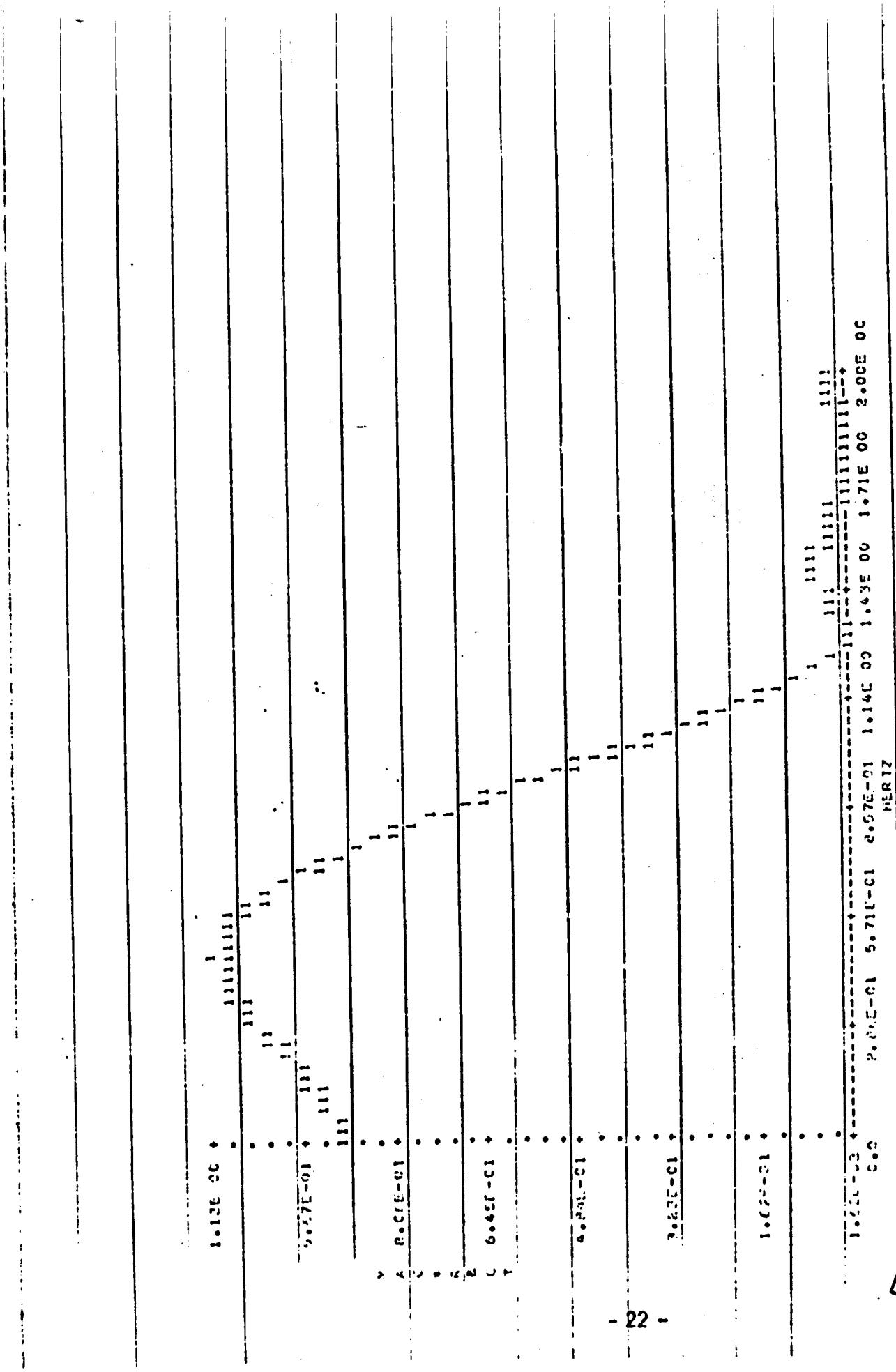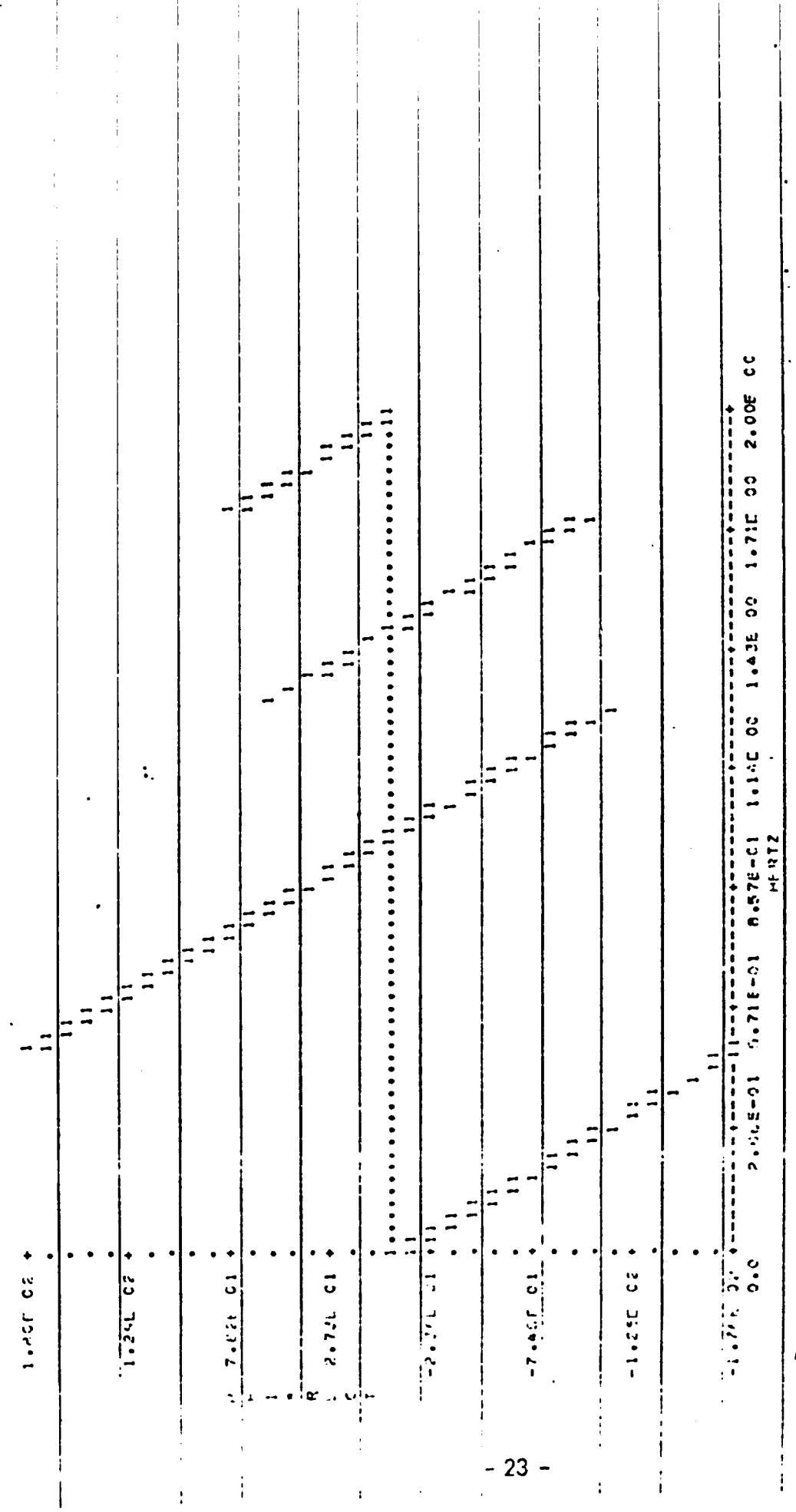
Figure 7. Rectangularly Weighted Filter Phase Response

- 23 -

BAND PASS TRANSVERSAL FILTERS

A low-pass to band-pass digital filter transformation may be effected by a technique which parallels that of a heterodyning process in analog signal theory. Performing this transformation on transversal filters allows the stability and well-behaved characteristics of this mechanization to be realized for the band-pass case. This straightforward transformation is achieved in the Z-domain by the following algorithm which mathematically converts the low-pass filter multiplier coefficients, a_n, to band-pass multiplier coefficients, A_n.

$$H_{LP}(Z) = \sum_{n=0}^{m} a_n Z^{-n} \tag{24}$$

$$H_{BP}(Z) = \frac{H_{LP}(Z e^{i\omega_o T}) + H_{LP}(Z e^{-i\omega_o T})}{Z} \tag{25}$$

$$= \sum_{n=0}^{m} A_n Z^{-n} \tag{26}$$

$$A_n = \sum_{r=0}^{m} a_{n-r} \cdot \cos [\omega_o T(n-2r)] \tag{27}$$

where ω_o is the filter center frequency. Derivation of the band-pass coefficients from Equation (27) requires close attention to the subscripts on the coefficient a_{n-r}. Note that the summation of terms on r for conversion of the low-pass filter coefficients, a_n, to the band-pass coefficients, A_n, is continued only until n = r. Negative subscript values are thereby precluded.

BAND PASS DESIGN EXAMPLE

Consider a band-pass filter based on the preceding low-pass transversal design with the purpose of providing DC attenuation while passing slowly varying AC components. A center frequency of 2 Hertz is chosen in the example at hand. Equation (28) provides coefficient conversion of the previous 17 low-pass Hamming-weighted coefficients with the same sampling time of $T = 1/8$ second.

$$A_n = \sum_{r=0}^{16} a_{n-r} \cdot \cos[\pi/2 \ (n-2r)] \qquad (28)$$

$A_0 = 0$ $A_4 = +.0004$ $A_8 = +.0554$ $A_{12} = 0.1596$

$A_1 = 0$ $A_5 = 0$ $A_9 = 0$ $A_{13} = 0 = A_{15}$

$A_2 = -.0044$ $A_6 = -.1279$ $A_{10} = +.1026$ $A_{14} = +.1445$

$A_3 = 0$ $A_7 = 0$ $A_{11} = 0$ $A_{16} = -.1592$

Figures 8 and 9 present the magnitude and phase response also generated by computer methods utilizing Equations (22) and (23) as before. Both passband and stopband ripple is in evidence even though conversion was effected from Hamming-weighted coefficients. This anomaly is characteristic of this method of generating a band-pass characteristic. Ripple reduction to a specific acceptable level is achieved as a trade-off with filter sampling rate in the same manner as for the low-pass design. Again, from Equation (18) it is apparent that the faster the sampling rate the greater the number of filter states, hence coefficients and delays, and thereby the more closely the filter realization will approximate the desired characteristic. In the example at hand 12 DB attenuation is achieved at DC. However, it is apparent that a judicious selection of
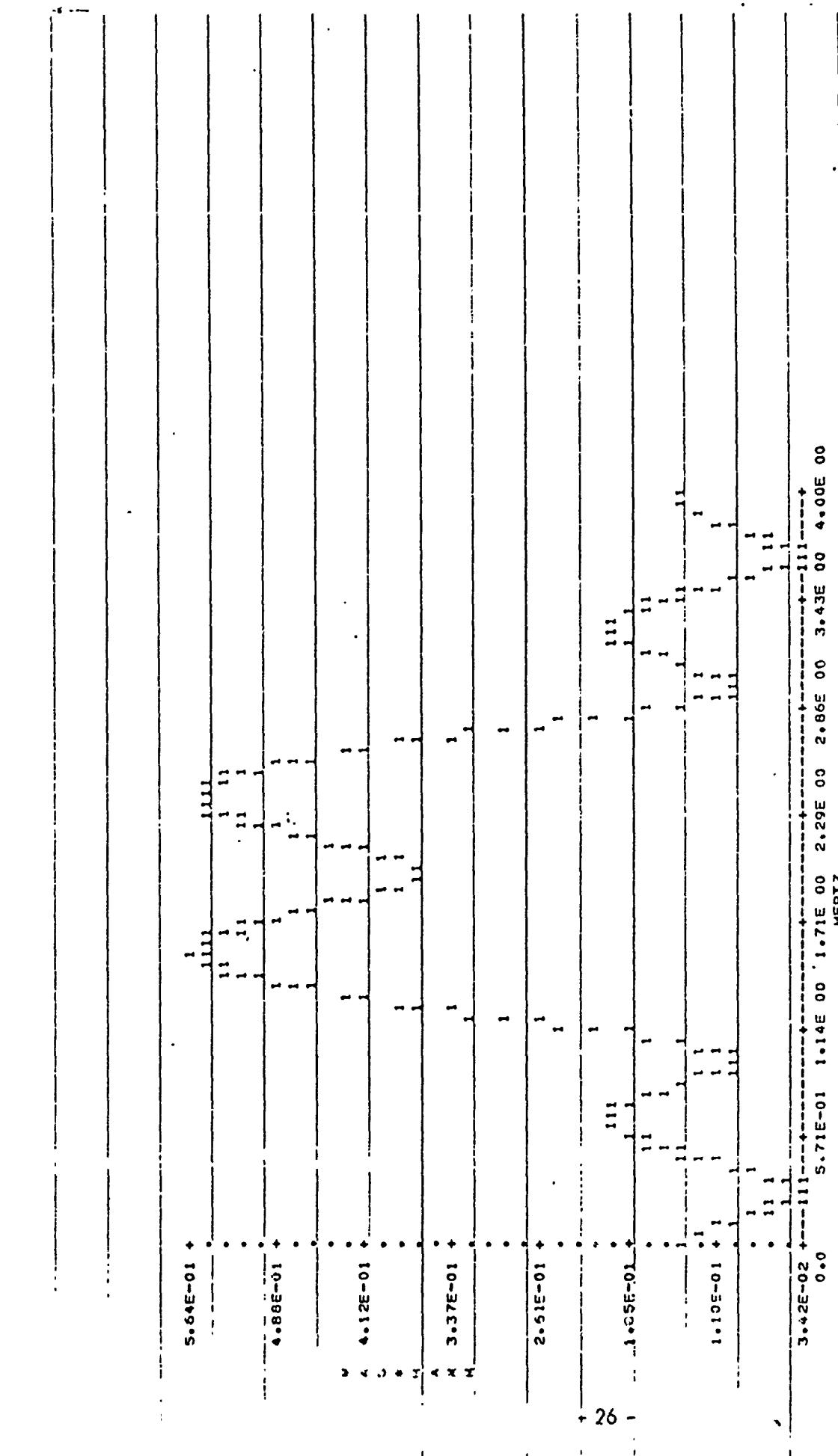
Figure 8. Hamming Weighted Filter Magnitude Response
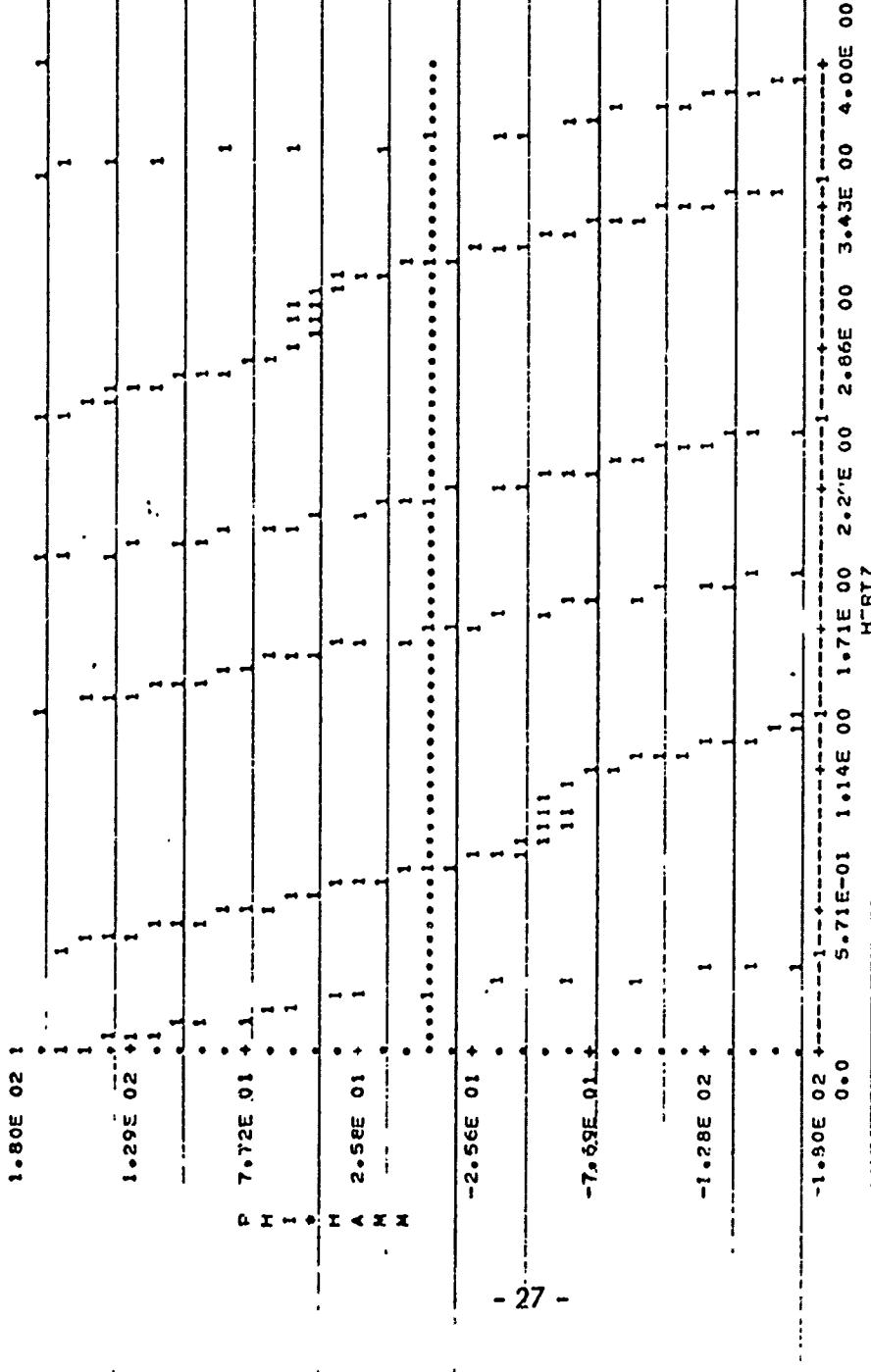
Figure 9. Hamming Weighted Filter Phase Response

filter center frequency, such as 1.6 Hertz, will place the stopband null of Figure 8

at DC for 24 DB rejection. The phase response in the filter passband i found to be

reasonably linear as shown by Figure 9. The phase warp shown occurs innocuously

at the nulls of the stopband.

BIBLIOGRAPHY

"IEEE Transactions on Audio and Electroacoustics", Volume AU-17, No. 2, June 1969.

Gold, B., and C. M. Rader, "Digital Processing of Signals", McGraw-Hill, New York, New York, c. 1969.

Oppenheim, A. V., "Papers on Digital Signal Processing", M.I.T. Press, Cambridge, Massachusetts, c. 1969.

Huelsman, L. P., "Active Filters: Lumped, Distributed, Integrated, Digital, and Parametric", McGraw-Hill, New York, New York, c. 1970.